

## Supporting Information

### Experimental

#### Preparation of well-dispersed magnetite (Fe<sub>3</sub>O<sub>4</sub>) particles.

Briefly, 10.25 g of FeCl<sub>3</sub>·6H<sub>2</sub>O and 10.0 g of sodium acetate were dissolved in 200 mL of ethylene glycol under vigorous stir, followed by the addition of polyethylene glycol (PEG, MW 2000) 2.5 g and sonication for 1 h. The resulting homogeneous yellow solution (90 mL) was transferred to a Teflon-lined stainless-steel autoclave (120 mL capacity). The autoclave was sealed and heated at 200 °C for 12 h and then naturally cooled to room temperature. The black Fe<sub>3</sub>O<sub>4</sub> particles were collected with the help of a magnet, followed by washing six times with ethanol and deionized water, and finally dried at 60 °C overnight.

#### Synthesis of Ln(OH)CO<sub>3</sub> (Ln=Er,Tm,Yb,Lu) particles.

The precursor particles of Ln(OH)CO<sub>3</sub> were prepared by the chemical precipitation method in accordance with the following procedure: First, Ln(NO<sub>3</sub>)<sub>3</sub> aqueous solution (0.25 M, 1.0 mL) and urea (1.0 g) were dissolved into deionized water (50 mL), followed by ultrasonication for 10 min. Subsequently, the mixture was magnetically stirred for 2 h in a water bath maintained at 90 °C. The resulting particles were collected after centrifugation and washed with deionized water, and then dried at 60 °C overnight.

#### Synthesis of xNH<sub>4</sub>F·yLnF<sub>3</sub> (Ln=Er,Tm,Yb) products using Ln(OH)CO<sub>3</sub> particles as precursors.

Ln(OH)CO<sub>3</sub> particles (18 mg) were dispersed into deionized water (50 mL) by ultrasonication for 10 min, followed by the addition of NH<sub>4</sub>F (2 mmol). Then the suspension solution was mechanically stirred for 2 h at 70 °C. The obtained NH<sub>4</sub>LnF<sub>x</sub> products were collected, washed with ethanol and water, and then dried at 60 °C overnight.

#### Preparation of Tryptic Digests of Standard Proteins.

β-casein and BSA (1 mg) were each dissolved in NH<sub>4</sub>HCO<sub>3</sub> solution (50mM, 1 mL). Protein solutions were then incubated with trypsin at an enzyme/substrate ratio of 1:50 (w/w) for 16 h at 37 °C to produce proteolytic digests. The tryptic peptide mixtures were stored at -20 °C until further use.

#### Preparation of Tryptic Digest of Proteins in Nonfat Milk.

For in-solution digestion, nonfat milk (30 μL) was first denatured by the ammonium bicarbonate solution (50 mM, 250 μL) containing urea (8 M) and incubated at 37 °C for 30 min. Then, DTT (Dithiothreitol) solution (200 mM, 25 μL) was introduced, and the temperature was maintained at

55 °C for 1 h. After cooled to room temperature, the IAA (Indole-3-acetic acid) solution (200 mM, 50 µL) was added and the mixture was kept in the dark for 3 h. Finally, the resulting sample was diluted to 1 mL with the ammonium bicarbonate solution (50 mM) and incubated with trypsin (2 mg/mL, 10 µL) at 37 °C for 18 h. The tryptic peptide mixtures were stored at -20 °C until further use.

### **Sample Preparation of Human Serum.**

Blood sample donated by a healthy person was collected in 5 mL amounts, allowed to clot at room temperature for up to 1 h, and centrifuged for 5 min at 1000 rpm. Sera (upper phase) were aliquoted and stored frozen box at -20°C. Before use, 10 µL of the serum sample was diluted with 900 µL of 50% (v/v) acetonitrile aqueous solution containing 0.1% TFA, and without any other purification and tedious treatment, the serum sample was ready for enrichment.

### **A more detailed explanation on the possible formation mechanism of the flowerlike $\gamma\text{-Fe}_2\text{O}_3@x\text{NH}_4\text{F}\cdot y\text{LuF}_3$ core-shell microspheres**

A possible mechanism involved the phase transformation reaction and the self-assembly growth in situ was proposed to account for the formation of the flowerlike  $\gamma\text{-Fe}_2\text{O}_3@x\text{NH}_4\text{F}\cdot y\text{LuF}_3$  core-shell microspheres. We guess that in the process of the phase transformation reaction, the  $\text{O}^{2-}$  in  $\text{Lu}_2\text{O}_3$  was first replaced by  $\text{F}^-$  ions via an ion-exchange reaction due to stronger interaction between  $\text{Lu}^{3+}$  and  $\text{F}^-$ , and the excess  $\text{F}^-$  ions simultaneously coordinated with  $\text{Lu}^{3+}$  to form coordination anions  $[\text{LuF}_x^{(x-3)-}]$ , then the  $\text{LuF}_x^{(x-3)-}$  coordination anions further reacted with  $\text{NH}_4^+$  through electrostatic attraction to form  $x\text{NH}_4\text{F}\cdot y\text{LuF}_3$  species, and finally the  $x\text{NH}_4\text{F}\cdot y\text{LuF}_3$  species became crystal nuclei for self-assembly growth. In the course of the self-assembly growth in situ, the  $x\text{NH}_4\text{F}\cdot y\text{LuF}_3$  crystal nuclei quickly grew up to form some scraggly interlaced 2D thin nanosheets, and simultaneously accompanied by the gradual etching of the  $\text{Lu}_2\text{O}_3$  shells which provide the  $\text{Lu}^{3+}$  resources. Subsequently these 2D epitaxial nanosheets gradually became bigger and bigger along independent directions until the  $\text{Lu}^{3+}$  resources were exhausted, and spontaneously in-situ self-assembled into 3D hierarchical shells.

Figures:

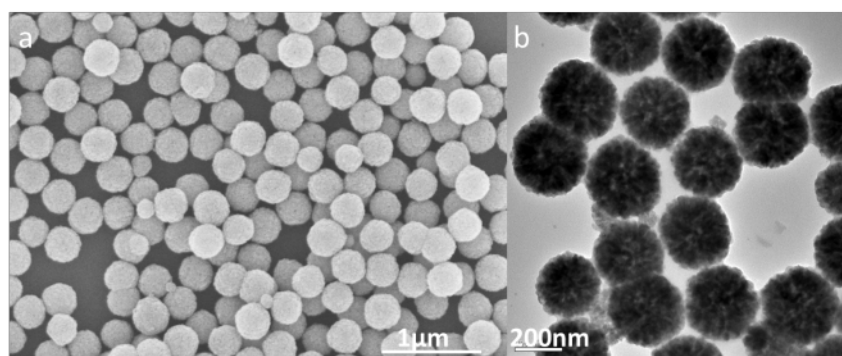


Fig. S1. a) SEM and b) TEM images of the pristine Fe<sub>3</sub>O<sub>4</sub> particles.

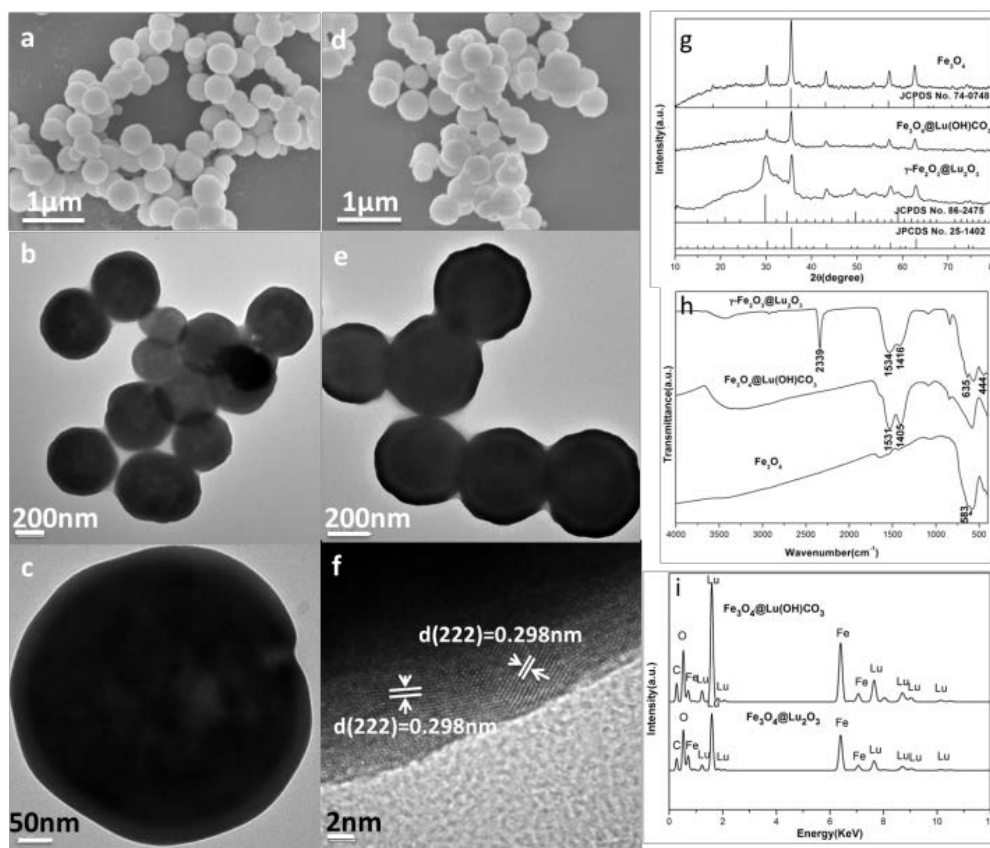
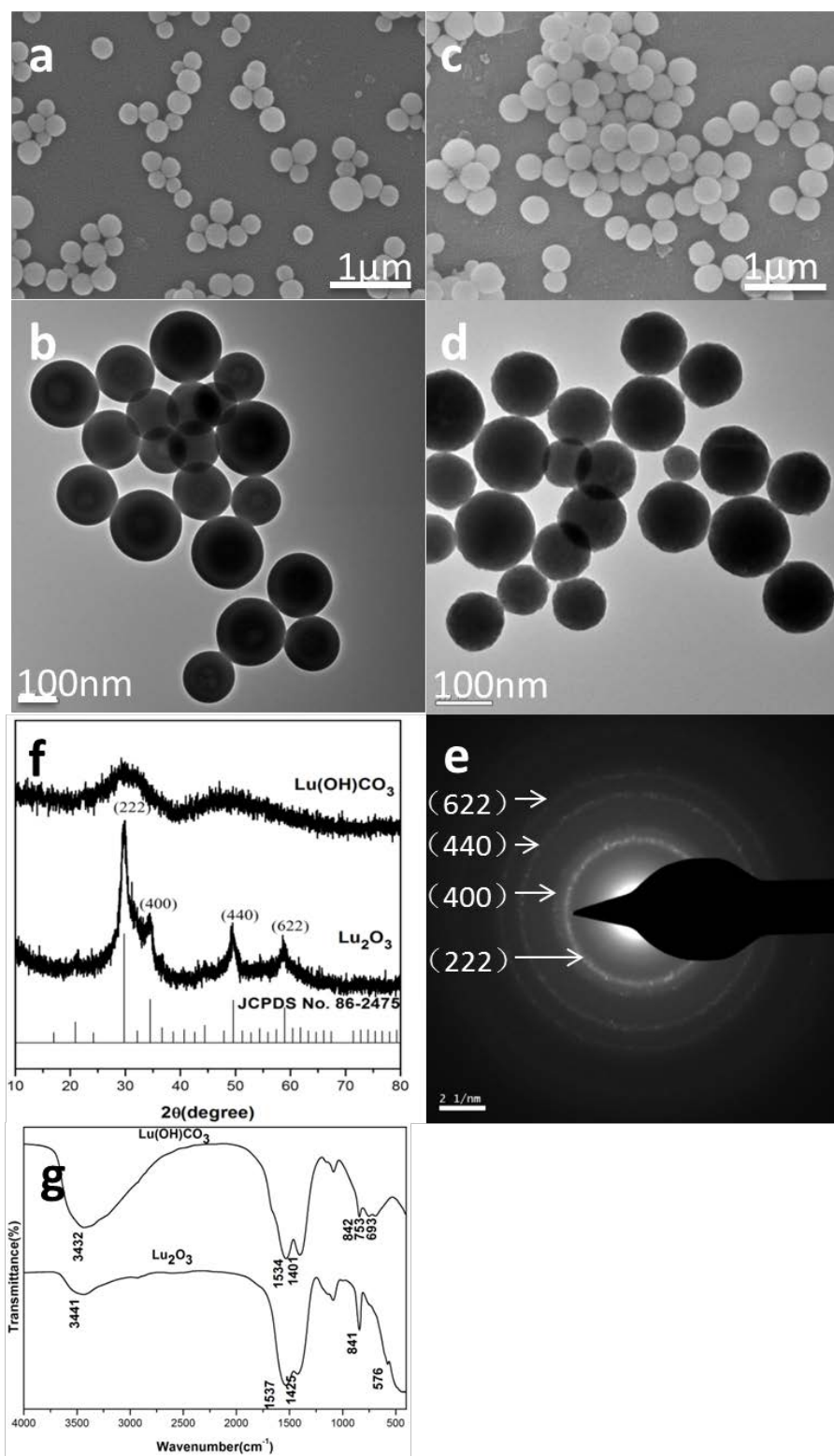


Fig. S2. Characterization of Fe<sub>3</sub>O<sub>4</sub>@Lu(OH)CO<sub>3</sub> and γ-Fe<sub>2</sub>O<sub>3</sub>@Lu<sub>2</sub>O<sub>3</sub> microspheres: a) SEM, b and c) TEM images of the Fe<sub>3</sub>O<sub>4</sub>@Lu(OH)CO<sub>3</sub> microspheres; d) SEM, e) TEM and f) HRTEM images of the γ-Fe<sub>2</sub>O<sub>3</sub>@Lu<sub>2</sub>O<sub>3</sub> microspheres; g) XRD patterns and h) FTIR spectra of the Fe<sub>3</sub>O<sub>4</sub>, Fe<sub>3</sub>O<sub>4</sub>@Lu(OH)CO<sub>3</sub> and γ-Fe<sub>2</sub>O<sub>3</sub>@Lu<sub>2</sub>O<sub>3</sub> microspheres; i) EDS spectra of the Fe<sub>3</sub>O<sub>4</sub>@Lu(OH)CO<sub>3</sub> and the γ-Fe<sub>2</sub>O<sub>3</sub>@Lu<sub>2</sub>O<sub>3</sub> microspheres.



**Fig. S3** Characterizations of Lu(OH)CO<sub>3</sub> and Lu<sub>2</sub>O<sub>3</sub> microspheres: a) SEM image of Lu(OH)CO<sub>3</sub> obtained through an urea-based homogeneous precipitation reaction. b) TEM image of Lu(OH)CO<sub>3</sub>. c) SEM image of Lu<sub>2</sub>O<sub>3</sub> obtained from the calcination treatment of Lu(OH)CO<sub>3</sub> at 550 °C for 2 h. d) TEM image of Lu<sub>2</sub>O<sub>3</sub>. e) Selected Area Electron Diffraction (SAED) image of Lu<sub>2</sub>O<sub>3</sub>, indicating the Lu<sub>2</sub>O<sub>3</sub> microspheres are polycrystalline. f) XRD patterns of the

Lu(OH)CO<sub>3</sub> and Lu<sub>2</sub>O<sub>3</sub> microspheres. g) FTIR spectra of the Lu(OH)CO<sub>3</sub> and Lu<sub>2</sub>O<sub>3</sub> microspheres.

Note: After the calcination treatment at 550 °C, the Fe<sub>3</sub>O<sub>4</sub> cores were transformed into  $\gamma$ -Fe<sub>2</sub>O<sub>3</sub>, and the Lu(OH)CO<sub>3</sub> shells were decomposed into Lu<sub>2</sub>O<sub>3</sub>, CO<sub>2</sub> and H<sub>2</sub>O. Some CO<sub>2</sub> molecules can be inevitably adsorbed by the magnetic cores due to the strong interaction between CO<sub>2</sub> and iron ions under the high temperature [ref. 44]. Thus, it can infer that the CO<sub>2</sub> molecules were mainly adsorbed by the magnetic cores rather than be included in the shells. The reasons are as follows. Firstly, after the calcination, the adsorption peak at 2339 cm<sup>-1</sup> clearly appear in the FTIR spectrum of  $\gamma$ -Fe<sub>2</sub>O<sub>3</sub>@Lu<sub>2</sub>O<sub>3</sub>, while it can not be observed in the FTIR spectrum of precursor Fe<sub>3</sub>O<sub>4</sub>@Lu(OH)CO<sub>3</sub> (Fig. S2h). This indicates that the CO<sub>2</sub> is derived from thermo-decomposition of the Lu(OH)CO<sub>3</sub>. Secondly, no CO<sub>2</sub> adsorption peak at 2337 cm<sup>-1</sup> can be observed in the FTIR spectra of Lu<sub>2</sub>O<sub>3</sub> obtained from the decomposition of Lu(OH)CO<sub>3</sub> microspheres (see Fig. S3), which indicated that all of the CO<sub>2</sub> produced by thermo-decomposition of the Lu(OH)CO<sub>3</sub> was released into the air in the absence of magnetic cores. Finally, the flowerlike product prepared by the precursor Fe<sub>3</sub>O<sub>4</sub>@Lu(OH)CO<sub>3</sub>, no CO<sub>2</sub> adsorption peak at 2337 cm<sup>-1</sup> can be observed in the FTIR spectrum of the flowerlike product (see Fig. 6). Based on the above analysis, we believe that the CO<sub>2</sub> produced from the decomposition of Lu(OH)CO<sub>3</sub> and was mainly adsorbed by the magnetic cores.

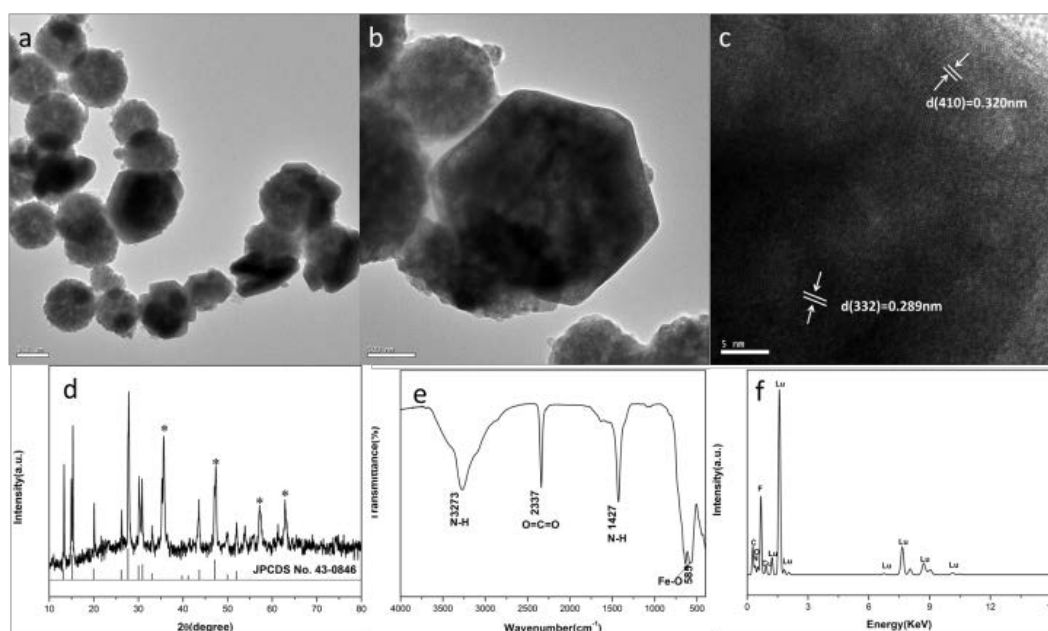


**Fig. S4** a, b) TEM images, d) XRD pattern and e) FTIR spectra of the  $\gamma$ -Fe<sub>2</sub>O<sub>3</sub>/NH<sub>4</sub>Lu<sub>2</sub>F<sub>7</sub> conjugate; c) HRTEM image and f) EDS of the NH<sub>4</sub>Lu<sub>2</sub>F<sub>7</sub> blocky particle.  $\gamma$ -Fe<sub>2</sub>O<sub>3</sub>@Lu<sub>2</sub>O<sub>3</sub> microspheres (30 mg) were used as precursor. The amount of NH<sub>4</sub>F is 30 mmol and the ion-exchange reaction temperature is 70 °C. \* indicates the diffraction peaks of  $\gamma$ -Fe<sub>2</sub>O<sub>3</sub>.

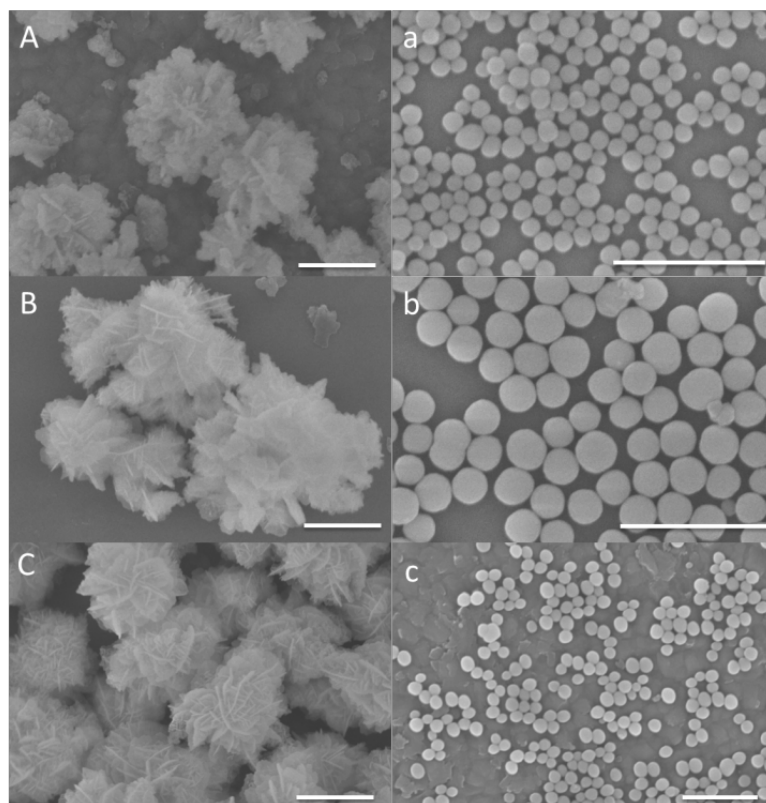


**Fig. S5** Representative SEM images of ion-exchange products: A)  $x\text{NH}_4\text{F}\cdot y\text{ErF}_3$ , B)  $x\text{NH}_4\text{F}\cdot y\text{TmF}_3$  and C)  $x\text{NH}_4\text{F}\cdot y\text{YbF}_3$  obtained under controlled conditions from a)  $\text{Er}(\text{OH})\text{CO}_3$ , b)  $\text{Tm}(\text{OH})\text{CO}_3$  and c)  $\text{Yb}(\text{OH})\text{CO}_3$  microspheres, respectively. Amount of the  $\text{Ln}(\text{OH})\text{CO}_3$  ( $\text{Ln}=\text{Er}$ ,  $\text{Tm}$ ,  $\text{Yb}$ ) precursor and the amount of  $\text{NH}_4\text{F}$  is 18 mg and 2 mmol, respectively. The phase transformation reaction temperature is 70 °C. (All scale bars are 1  $\mu\text{m}$ )

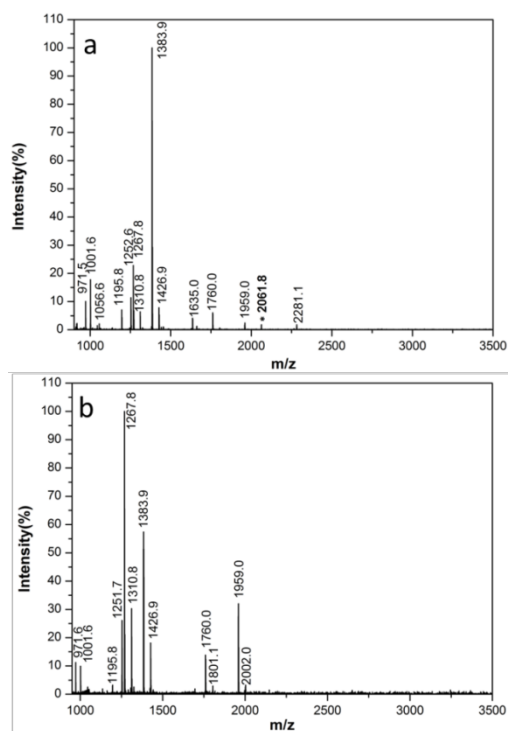


**Fig. S6** MALDI-TOF mass spectra of a)  $\beta$ -casein digest ( $5 \times 10^{-7}$  M), b) the tryptic digests of the nonfat milk treated without the  $\gamma\text{-Fe}_2\text{O}_3 @ x\text{NH}_4\text{F} \cdot y\text{LuF}_3$  affinity microspheres.

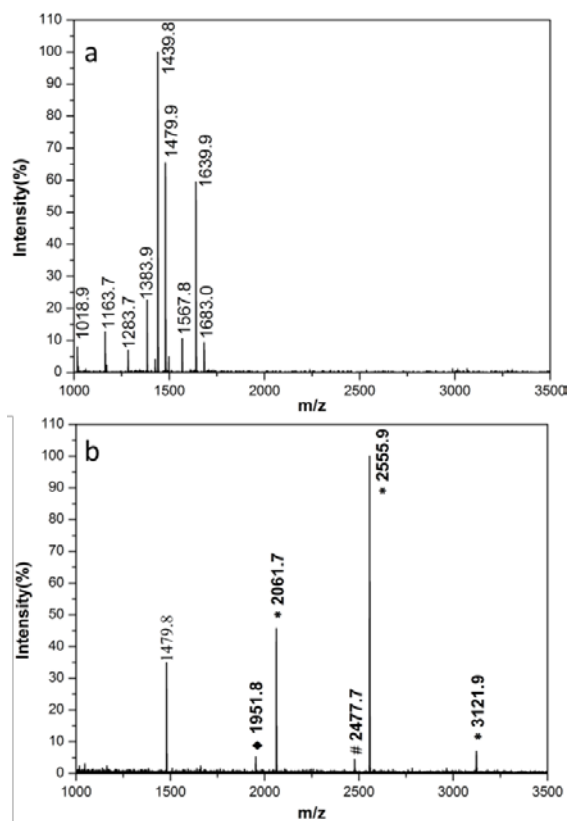


**Fig. S7** MALDI-TOF spectra of peptides from a mixture of  $\beta$ -casein and BSA (1:10, molar ratio) a) before and b) after treatment with  $\gamma\text{-Fe}_2\text{O}_3 @ x\text{NH}_4\text{F} \cdot y\text{LuF}_3$ . \* indicates phosphorylated peptides, # indicates their dephosphorylated and dehydration counterparts, and  $\blacklozenge$  indicates the phosphopeptides from  $\alpha$ -casein.

Table S1. The phosphopeptides captured by  $\gamma\text{-Fe}_2\text{O}_3 @ \text{xNH}_4\text{F} \cdot \text{yLuF}_3$  from tryptic digest of  $\beta$ -casein.

No.	[M+H] <sup>+</sup>	Protein	Phosphorylation site	Amino acid sequence
1	2061.9	$\beta$ -casein	1	FQ[pS]EEQQQTELQDK
2	2556.0	$\beta$ -casein	1	FQ[pS]EEQQQTEDELQDKIHPF
3	3122.3	$\beta$ -casein	4	ELEELNVPGEIVE[pS]L[pS][pS][pS]EESITR

Table S2. The phosphopeptides captured by  $\gamma\text{-Fe}_2\text{O}_3 @ \text{xNH}_4\text{F} \cdot \text{yLuF}_3$  from tryptic digest of non-fat milk.

No.	[M+H] <sup>+</sup>	Protein	Phosphorylation site	Amino acid sequence
1	1660.8	$\alpha$ S1-casein	1	VPQLEIVPN[pS]AEER
2	1927.7	$\alpha$ S1-casein	2	DIG[pS]E[pS]TEDQAMEDIK
3	2061.9	$\beta$ -casein	1	FQ[pS]EEQQQTELQDK
4	2886.5	$\beta$ -casein	3	ELEELNVPGEIVESL[pS][pS][pS]EESITR
5	2966.2	$\beta$ -casein	4	ELEELNVPGEIVE[pS]L[pS][pS][pS]EESITR
6	3009.1	$\alpha$ S2-casein	4	NANEEEEYSIG[pS][pS][pS]EE[pS]AEVATEEVK
7	3122.3	$\beta$ -casein	4	ELEELNVPGEIVE[pS]L[pS][pS][pS]EESITR

Table S3. The phosphopeptides captured by  $\gamma\text{-Fe}_2\text{O}_3 @ \text{xNH}_4\text{F} \cdot \text{yLuF}_3$  from human serum.

No.	[M+H] <sup>+</sup>	Phosphorylation site	Amino acid sequence
HS1	1545.8	1	D[pS]GEGDFLAEGGGVR
HS2	1616.9	1	AD[pS]GEGDFLAEGGGVR